PARAMETER IDENTIFICATION OF A HYBRID REDUNDANT ROBOT BY USING DIFFERENTIAL EVOLUTION ALGORITHM

Yongbo Wang, Huapeng Wu and Heikki Handroos

Department of Mechanical Engineering, IMVE, Lappeenranta University of Technology, Lappeenranta, Finland

Keywords: Calibration, Parameter Identification, Parallel Robot, Differential Evolution.

Abstract: In this paper, a hybrid redundant robot IWR (Intersector Welding Robot) which possesses ten degrees of freedom (DOF) where 6-DOF in parallel and additional redundant 4-DOF in serial is proposed. To improve the accuracy of the robot, the kinematic errors caused by the manufacturing and assembly processes have to be compensated or limited to a minimum value. However, currently, there is no effective instrument which capable of measuring the symmetrical errors of the corresponding joints and link lengths after the structure has been assembled. Therefore, calibration and identification of these unknown parameters is utmost important and necessary to the systematic accuracy. This paper presents a calibration method for identifying the unknown parameters by using differential evolution (DE) algorithm, which has proven to be an efficient, effective and robust optimization method to solve the global optimization problems. The DE algorithm will guarantee the fast convergence and accurate solutions regardless of the initial conditions of the parameters. Based on the inverse kinematic error model of the robot, the simulation of the actual robot is achieved by introducing random geometric errors and measurement poses which representing their relative physical behavior. Moreover, through computer simulation, the validity and effectiveness of the DE algorithm for the parameter identification of the proposed application has also been examined.

1 INTRODUCTION

It is widely believed that parallel robot has high stiffness, low inertia, high speed and accuracy but small workspace compared to its counterpart serial robot. To take advantage of the benefits (bigger workspace and higher stiffness) of both types of robotic structures, a compromised hybrid redundant robot which can be used to perform the welding, machining and remote handling is developed in Lappeenranta University of Technology (Wu, 2005). In order to satisfy the required accuracy of the robot, the calibration and identification of the real structure parameters is essential and necessary. Generally, calibration can be classified into two types: static and dynamic. The static or kinematic calibration is an identification of those parameters which influence primarily the static positioning characteristics of a robot, such as the errors caused by length of the links and joints. Whereas the dynamic calibration is used to identify parameters influencing primarily motion characteristics, such as the deflection of mechanisms caused by temperature, and the compliances of joints and links. This paper will be concentrated on the static calibration to identify the geometric parameters of the proposed hybrid redundant robot. At present, there exist two kinds of static or kinematic calibration methods, one is self or autonomous calibration method based on inner information or restrictions of the kinematic parameters of joints (Ryu, 2001; Zhuang, 1996; Khalil, 1999; Zhuang, 2000; Ecorchard, 2005), and another is exterior or classical calibration method by using accurate instruments to measure the pose of the moving platform directly (Gao, 2003; Besnard, 1999; Prenaud, 2003). For these calibration methods, most of them are focused on the kinematic calibration and parameter identification of the pure-serial or pure-parallel mechanisms. Moreover, many calibration models are based on the identification Jacobian matrix which formulates a linear relationship between measurement residuals and kinematic parameter errors, then the parameter errors are evaluated by using least square algorithm. However, this kind of method is subject to break down in the vicinity of singular robot configurations due to the iterative inversion of the robot Jacobian (Zhong, 1996). Instead of the Jacobian matrix based

Wang Y., Wu H. and Handroos H. (2009).
PARAMETER IDENTIFICATION OF A HYBRID REDUNDANT ROBOT BY USING DIFFERENTIAL EVOLUTION ALGORITHM.
In *Proceedings of the 6th International Conference on Informatics in Control, Automation and Robotics - Robotics and Automation*, pages 287-292
DOI: 10.5220/0002214202870292

calibration approaches, the non-parametric calibration method was introduced by Shamma and Whitney (Shamma, 1987), in which the actual kinematic parameters which drive the robot to minimize the end-effector deviations can be found by using non-linear least-square optimization without explicit evaluation of the Jacobian. Based on the non-parametric calibration method, some evolutionary computing algorithms, such as genetic algorithm (GA) (Liu, 2007; Zhuang, 1996), artificial neural networks (NN) (Zhong,1996) and genetic programming (GP) (Dolinsky, 2007), have been successfully employed to calibrate serial or parallel robot. Differential evolution (DE) is a simple but effective evolutionary algorithm for solving non-linear, global optimization problems. It has demonstrated superior performance in both widely used benchmark functions (Vesterstrom, 2004) and practical applications (Wu, 2000). In this work, based on the static and non-parametric calibration method, DE will be adopted to identify the real kinematic parameters of the proposed hybrid redundant robot.

The paper is organized into five main sections. The first section serves as an introduction. The second section reviews the kinematic model of the proposed robot, which includes the inverse kinematic equations and the error models of the robot. Section 3 presents the calibration equations and the implement of DE optimization method. Simulation results are presented in section 4, and conclusions are drawn in section 5.

2 IDENTIFICATION MODELS

The kinematics of the proposed hybrid robot as shown in Fig.1 is a combination of a multi-link serial mechanism (here named as Carriage) and a standard Stewart parallel manipulator (here named as Hexa-WH). To simplify its analysis, the two parts will be first carried out separately, and then combined them together to obtain the final solutions. According to Shamma and Whitney (Shamma, 1987), the calibration also can be classified into forward calibration and inverse calibration. Forward calibration involves finding the actual location in the world space for a given joint configuration, while inverse calibration involves finding exact joint values for given locations in the world space. As we all know that the inverse kinematics of the parallel robot is simple than forward kinematics and vice versa for the serial robot, so we decide to identify the kinematic parameters of the parallel part based on inverse calibration method and the serial part based on forward solutions

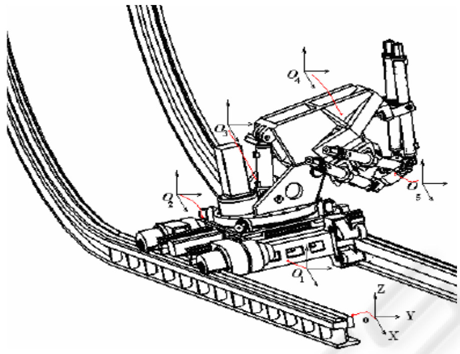

Figure 1: 3D model of IWR.

2.1 Forward Kinematics

To study the kinematics of the serial multi-link mechanisms, the convention of Denavit-Hartenberg (Craig, 1986) is commonly adopted. Based on this convention, the principle of the 4-DOF Carriage mechanism can be established as shown in Fig.2, which provides four degrees of freedom to the transient end-effector (O_4), including two translational movements and two rotational movements.

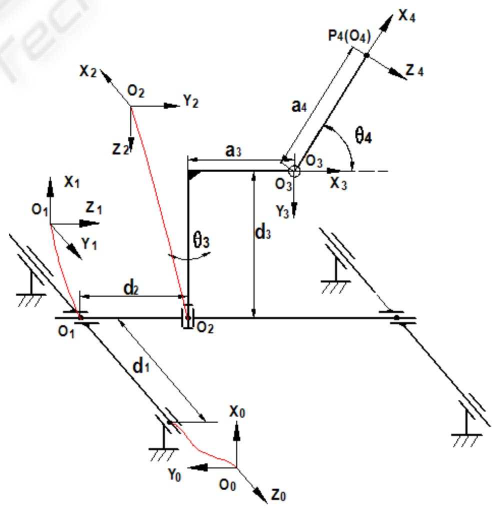

Figure 2: Coordinate system of Carriage.

Using the coordinate systems established in Fig. 2, the corresponding link parameters are given in Table1. Substituting the D-H link parameters into (1), we can obtain the D-H homogeneous transformation matrices ${}^0\mathbf{A}_1, {}^1\mathbf{A}_2, {}^2\mathbf{A}_3, {}^3\mathbf{A}_4$.

Table 1: Nominal DH parameters of Carriage.

Joint	α_i	a_i	d_i	θ_i
1	$\pi/2$	0	d_1	0
2	$\pi/2$	0	d_2	$\pi/2$
3	$\pi/2$	a_3	d_3	θ_3
4	$-\pi/2$	a_4	0	θ_4

$$ {}^{i-1}\mathbf{A}_i = \begin{bmatrix} c\theta_i & -c\alpha_i s\theta_i & s\alpha_i s\theta_i & a_i c\theta_i \\ s\theta_i & c\alpha_i c\theta_i & -s\alpha_i c\theta_i & a_i s\theta_i \\ 0 & s\alpha_i & c\alpha_i & d_i \\ 0 & 0 & 0 & 1 \end{bmatrix} \quad (1) $$

where $c\theta_i$ denotes $\cos\theta_i$, and $s\theta_i$ denotes $\sin\theta_i$.

The resulting homogeneous transformation matrix, i.e. the forward kinematics of the Carriage, can be obtained by multiplying the matrices of ${}^0\mathbf{A}_1$,${}^1\mathbf{A}_2$,${}^2\mathbf{A}_3$ and ${}^3\mathbf{A}_4$

$$ {}^0\mathbf{A}_4 = {}^0\mathbf{A}_1 {}^1\mathbf{A}_2 {}^2\mathbf{A}_3 {}^3\mathbf{A}_4 = \begin{bmatrix} s\theta_4 & 0 & c\theta_4 & a_1 + d_3 + a_4 s\theta_4 \\ -s\theta_3 c\theta_4 & -c\theta_3 & s\theta_3 s\theta_4 & -d_2 - a_3 s\theta_3 - a_4 s\theta_3 c\theta_4 \\ c\theta_3 c\theta_4 & -s\theta_3 & -c\theta_3 s\theta_4 & d_1 + a_3 c\theta_3 + a_4 c\theta_3 c\theta_4 \\ 0 & 0 & 0 & 1 \end{bmatrix} \quad (2) $$

From (2) we can get the rotation matrix and position vector of the frame {4} with respect to frame {0} as follows:

$$ {}^0\mathbf{R}_4 = \begin{bmatrix} s\theta_4 & 0 & c\theta_4 \\ -s\theta_3 c\theta_4 & -c\theta_3 & s\theta_3 s\theta_4 \\ c\theta_3 c\theta_4 & -s\theta_3 & -c\theta_3 s\theta_4 \end{bmatrix} \quad (3) $$

$$ {}^0\mathbf{P}_4 = \begin{bmatrix} a_1 + d_3 + a_4 s\theta_4 \\ -d_2 - a_3 s\theta_3 - a_4 s\theta_3 c\theta_4 \\ d_1 + a_3 c\theta_3 + a_4 c\theta_3 c\theta_4 \end{bmatrix} \quad (4) $$

In reality, the above D-H parameters will deviate from their nominal values because of the manufacturing and assembly errors. Since each joint provides four parameters, therefore, the four links will produce 16 identified parameters for the robot.

2.2 Inverse Kinematics of Hexa-WH

Fig. 3 shows a schematic diagram of hexapod parallel mechanism, for the purpose of analysis, two Cartesian coordinate systems, frames $O_4(X_4, Y_4, Z_4)$ and $O_5(X_5, Y_5, Z_5)$ are attached to the base plate and the end-effector, respectively. Six variable limbs are connected with the base plate by Universal joints and the task platform by Spherical joints.

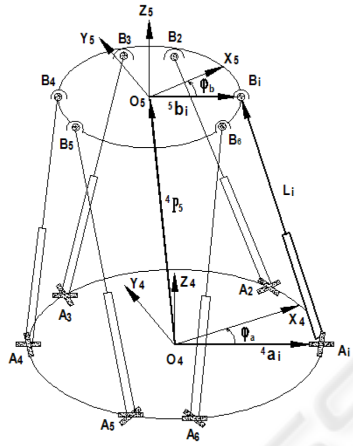

Figure 3: Norminal model of the Hexapod parallel mechanism.

For the designed kinematics parameters, let $\mathbf{l}_i$ be the unit vector in the direction of $\mathbf{A}_i\mathbf{B}_i$, and l_i denote the magnitude of the leg vector $\mathbf{A}_i\mathbf{B}_i$, then the following vector-loop equation will represent the inverse kinematics of the *ith* limb of the manipulator.

$$ l_i\mathbf{l}_i = {}^4\mathbf{P}_5 + {}^4\mathbf{R}_5\,{}^5\mathbf{b}_i - {}^4\mathbf{a}_i \qquad (i = 1,2,\cdots 6) \quad (5) $$

where ${}^4\mathbf{P}_5$ denotes the position vector of the task frame {5} with respect to the base frame {4}, and ${}^4\mathbf{R}_5$ is the Z-Y-X Euler transformation matrix expressing the orientation of the frame {5} relative to the frame {4},

$$ {}^4\mathbf{R}_5 = \begin{bmatrix} c\alpha c\beta & c\alpha s\beta s\gamma - s\alpha c\gamma & c\alpha s\beta c\gamma + s\alpha s\gamma \\ s\alpha s\beta & s\alpha s\beta s\gamma + c\alpha c\gamma & s\alpha s\beta c\gamma - c\alpha s\gamma \\ -s\beta & c\beta s\gamma & c\beta c\lambda \end{bmatrix} \quad (6) $$

and the ${}^4\mathbf{a}_i$, ${}^5\mathbf{b}_i$ represent the position vectors of U-joints $\mathbf{A}_i$ $\mathbf{A}_i$ and S-joints $\mathbf{B}_i$ in the coordinate frames {4} and {5} respectively. In practice, due to the manufacturing and assembly errors, the coordinate ${}^4\mathbf{a}_i$ and ${}^5\mathbf{b}_i$ will deviate from their nominal values and l_i will also have an initial offset, altogether there will be 42 identified parameters provided by Hexa-WH.

2.3 Kinematics and Identified Error Model of the Hybrid Manipulator

The schematic diagram of the redundant hybrid manipulator is shown in Fig. 4, which consists of

Carriage and Hexapod manipulator as mentioned above. The base plate frame {4} of Hexa-WH is coincided with the end task frame of Carriage. The global base frame {0} is located at the left rail of Carriage.

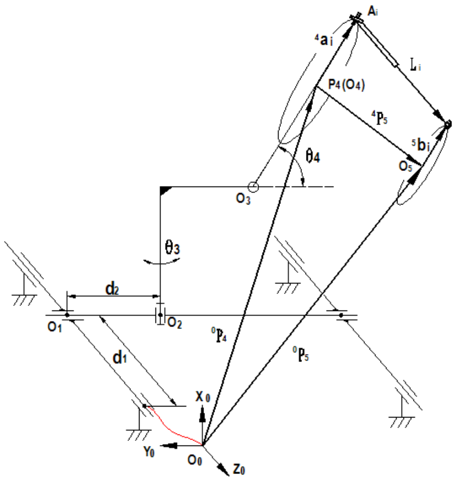

Figure 4: Schematic diagram of IWR.

According to the geometry, a vector-loop equation can be derived:

$$\begin{aligned} {}^0\mathbf{P}_5 &= {}^0\mathbf{P}_4 + {}^0\mathbf{R}_4\,{}^4\mathbf{P}_5 = {}^0\mathbf{P}_4 + {}^0\mathbf{R}_4\left(l_i\mathbf{l}_i + {}^4\mathbf{a}_i - {}^4\mathbf{R}_5\,{}^5\mathbf{b}_i\right) \\ &= {}^0\mathbf{P}_4 + {}^0\mathbf{R}_4 l_i\mathbf{l}_i + {}^0\mathbf{R}_4\,{}^4\mathbf{a}_i - {}^0\mathbf{R}_5\,{}^5\mathbf{b}_i \end{aligned} \quad (7)$$

From (7), we can obtain the nominal leg length, i.e. the inverse solution of the robot as:

$$l_i\mathbf{l}_i = \left({}^0\mathbf{R}_4\right)^{-1}\left({}^0\mathbf{P}_5 - {}^0\mathbf{P}_4 - {}^0\mathbf{R}_4\,{}^4\mathbf{a}_i + {}^0\mathbf{R}_5\,{}^5\mathbf{b}_i\right) \quad (8)$$

where ${}^0\mathbf{P}_5$ and ${}^0\mathbf{R}_5$ is the position vector and rotation matrix of the task frame {5} (or end-effector) with respect to the fixed base frame {0}.

Let l_i^m represent the whole leg length which made up of the measured leg length with the inner sensor and the fixed initial leg length offset. Therefore, if parameter errors are not be taken into account, there is the following relation.

$$l_i = l_i^m \quad (9)$$

As a matter of fact, since geometrical errors and other error sources exist, two sides of (9) will never be equal, even if their geometrical parameters are properly corrected. Consequently, if we get enough measurement point data from the inner sensors of the parallel Hexa-WH legs and the Carriage actuators, then our identified kinematic error model can be expressed as an optimization function given as follows:

$$\min \quad Fun(\delta\boldsymbol{\alpha}_c, \delta\mathbf{d}_c, \delta\mathbf{a}_c, \delta\boldsymbol{\theta}_c, \delta\mathbf{a}_h, \delta\mathbf{b}_h, \delta\mathbf{l}_h) = \sum_{i=1}^{N}\sum_{j=1}^{6}(l_{i,j} - l_{i,j}^m)^2 \quad (10)$$

where $\delta\boldsymbol{\alpha}_c, \delta\mathbf{d}_c, \delta\mathbf{a}_c, \delta\boldsymbol{\theta}_c, \delta\mathbf{a}_h, \delta\mathbf{b}_h, \delta\mathbf{l}_h$ denote the 58 identified parameter vectors, among which 16 parameters are from Carriage and 42 parameters from Hexa-WH. N is measurement number, $l_{i,j}$ and $l_{i,j}^m$ respectively represent the calculated value and measured value of the jth leg in the ith measurement point.

3 DIFFERENTIAL EVOLUTION

Differential Evolution (DE), which introduced by Price and Storn (Storn, 2005), has been proven to be a promising candidate for minimizing real-valued, non-linear and multi-modal objective functions. It belongs to the class of evolutionary algorithms and utilizes the same steps as Genetic Algorithm, i.e. mutation, crossover and selection. Individuals in DE are represented by D-dimensional vectors $\mathbf{x}_{i,G}$, $\forall i \in \{1,2,\cdots,NP\}$, where D is the number of optimization parameters and NP is the population size. There are several variants or strategies of DE, but the DE scheme which classified by notation DE/rand/1/bin is the most commonly used one. The optimization process of this classical DE can be summarized as follows:

3.1 Initialization

To establish a starting point for the optimization process, an initial population must be created. Typically, each decision parameter in every vector of the initial population is assigned by a randomly chosen value from its feasible bounds:

$$x_{j,i,G=0} = x_{j,i}^L + rand_j[0,1)\cdot(x_{j,i}^U - x_{j,i}^L) \quad (11)$$

where $j = 1,2,\cdots,D$ is parameter index, and $i = 1,2,\cdots,NP$ is population index, $x_{j,i}^L$ and $x_{j,i}^U$ are the lower and upper bound of the jth decision parameter, respectively. After the initial population has been created, it evolves through the following operations of mutation, crossover and selection until the terminal condition satisfied.

3.2 Mutation

For each vector $\mathbf{x}_{i,G}$, a mutant vector $\mathbf{m}_{i,G}$ is generated according to

$$\mathbf{m}_{i,G} = \mathbf{x}_{r1,G} + F \cdot (\mathbf{x}_{r2,G} - \mathbf{x}_{r3,G}) \tag{12}$$

where randomly selected integers $r_1, r_2, r_3 \in \{1,2,\cdots NP\}, r_1 \neq r_2 \neq r_3 \neq i$, and mutation scale factor $F > 0$.

3.3 Crossover

The trial vector is generated as follows:

$$\mathbf{u}_{i,G+1} = (u_{1,i,G+1}, u_{2,i,G+1}, \cdots, u_{D,i,G+1})$$

$$u_{j,i,G+1} = \begin{cases} m_{j,i,G+1} & if\ (rand_j[0,1) < CR \vee j = j_r) \\ x_{j,i,G+1} & otherwise, \end{cases} \tag{13}$$

where $G = 1,2,\cdots,G_{\max}$ denotes generation index, the index j_r is chosen randomly from the set $\{1,2,\cdots,D\}$, which is used to ensure that vector $\mathbf{u}_{j,i,G+1}$ gets at least one parameter from $\mathbf{m}_{i,G}$, and CR is known as a crossover rate constant which is a user-defined parameter within the range $[0,1]$.

3.4 Selection

To decide whether or not the trail vector should become a member of the next generation, the trail vector $\mathbf{u}_{i,G+1}$ is compared to the target vector $\mathbf{x}_{i,G}$ by evaluating the cost or objective function. A vector with a minimum value of cost function will be allowed to advance to the next generation. That is,

$$\mathbf{x}_{i,G+1} = \begin{cases} \mathbf{u}_{i,G+1} & if\quad fun(\mathbf{u}_{i,G+1}) \leq fun(\mathbf{x}_{i,G}), \\ \mathbf{x}_{i,G} & otherwise, \end{cases} \tag{14}$$

Using this selection procedure, all individuals of the next generation are as good as or better than the individuals of the current population.

4 SIMULATION RESULTS

To simulate the above process, we randomly generate 100 measurement poses within the robot workspace to form the measured input values. As stated above, we can take (10) as our fitness function, among which, we assume a set of fixed geometric errors for the identified parameter to represent the actual measurement values of the robot, and at the same time suppose these error parameters to be our simulation variables. Through enough evolution generations, the simulated identification parameter will finally approximate to the assumed parameter errors. Table 2 shows the constant parameters we have chosen and the best objective function values of each generation are plotted in Fig. 5.

Table 2: Parameters of DE.

Symbol	Parameter	Value
D	Number of parameters (Variables)	58
NP	Number of population	600
F	Scale or difference factor	0.9
CR	Crossover control constant	1.0
N	Measurement number	100
$G_{\max}$	The maximum generations	60000
$x_{j,i}^{L}$	Lower bound of identified error parameters	-0.5
$x_{j,i}^{U}$	Upper bound of identified error parameters	0.5

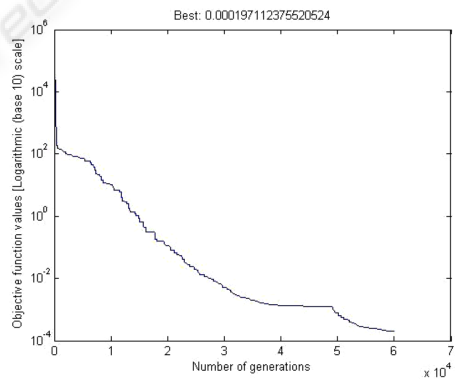

Figure 5: Best objective function values of 60000 generations.

From the above tables and the figure of evolutionary process, we can see that the objective function values decrease dramatically at the beginning, but with the advance of evolution process, they tend to be calm and the convergence speed also become slow. After 60000 generations, most of the identified errors are approximated to the assumed errors, and the final best object function value reach to the accuracy of 10^{-4}. Of course, if we increase the maximum generation number and add more measured poses, then the identification accuracy will be improved and the identified parameters will infinitely approach to the actual values.

5 CONCLUSIONS

In this paper, a hybrid redundant robot used for both machining and assembling of Vacuum Vessel of ITER is introduced. Furthermore, a parameter identification model which has the ability to account for the static error sources is derived. Due to the redundant freedom of the robot, we first divide the robot into two parts according to its mechanism, then formulate the parameter identification model respectively, and finally combine them together to get the final optimization identification model. Based on the DE algorithm and the derived identification model, the 58 kinematic error parameters of the robot were identified by computer simulations. According to the simulation results, we can see that DE has a very strong stochastic searching ability, which is reliable and can be easily used to identify the high non-linear kinematic error parameter models.

REFERENCES

Ecorchard, G.; Maurine, P, 2005. Self- calibratrion of delta parallel robots with elastic deformation compensation, *2005 IEEE/RSJ International Conference on Intelligent Robots and Systems, 2-6 Aug. 2005, pp, 1283 – 1288.*

Gao, Meng, Li Tiemin, Yin Wensheng, 2003. Calibration method and expriment of stewart platform using a laser tracker, *IEEE International Conference on Systems, Man and Cybernetics, Vol. 3, 5-8 Oct. 2003 pp. 2797 – 2802.*

Hanqi Zhuang, Jie Wu et al., 1996. Optimal Planning of Robot Calibration Experiments by Genetic Algorithms, *Proceedings of the 1996 IEEE International Conference on Robotics and Automation, Minneapolis, Minnesota, April 1996, pp. 981-986.*

Hanqi Zhuang, Lixin Liu, 1996. Self-calibration of a class of parallel manipulators, *Proceedings of the 1996 IEEE international conference on robotics and automation, Minneapolis, Minnesota, April 1996,pp.994-999.*

Hanqi Zhuang, Lixin Liu, Oren Masory, 2000. Autonomous calibration of hexapod machine tools, *ASME transactions on Journal of Manufacturing Science and Engineering, February 2000, Vol. 122, pp. 140-148.*

Huapeng Wu, Heikki Handroos, 2000. Utilization of differential evolution in inverse kinematics solution of a parallel redundant manipulator, *IEEE conference on knowledge-based intelligent engineering systems & allied technologies, 30 Aug. – 1 Sept. 2000, Brighton, UK, pp.812-815.*

Huapeng Wu, Heikki Handroos et al. 2005. Development and control towards a parallel water hydraulic weld/cut for machining processes in ITER vacuum vesse. *Int. J. fusion Engineering and Design, Vol. 75-79, pp. 625-631.*

J. Craig, 1986. *Introduction to Robotics: Mechanics and Control* , Addison-Wesley Publishing Co., Reading, MA.

J.Vesterstrom, R.Thomsen, 2004. A comparative study of differential evolution, particle swarm optimization, and evolutionary algorithms on numerical benchmark problems, *Evolutionary computation, Vol. 2. pp. 1980-1987.*

J.U. Dolinsky, I.D.Jenkinson et al., 2007. Application of Genetic Programming to the Calibration of Industrial Robots, *Journal of Computers in Industry, 58 (2007), pp. 255-264.*

Jeha Ryu, Abdul Rauf, 2001. A new method for fully autonomous calibration of parallel manipulators using a constraint link. *2001 IEEE/ASME international Conference on advanced intelligent mechatronics proceedings 8-12 July, 2001 Como, Italy, pp. 141-146.*

Prenaud and N. Andreff et al, 2003. Vision-based kinematic calibration of a H4 parallel mechanism, Proc. *IEEE Int. Conf. on Robotics and Automation, Taipei, Taiwan, pp.1191-1196.*

R. Storn and K. Price, 2005. *Differentila Evolution – a Practical Approach to Global Optimization*, Springer, Germany.

S.Besnard,W.Khalil, 1999. Calibration of parallel robots using two inclinometers, *Proceedings of the 1999 IEEE int. Conference on Robotics & Automation, Detroit, Michigan, pp.1758-1763.*

Shamma J.S. and Whitney D.E., 1987. A mehod for inverse robot calibration, *J. of Dynamic Systems, Measurement and Control. Vol, 109,pp.36-43.*

W. Khalil and S. Besnard, 1999. Self calibration of Stewart-Gough parallel robots without extra sensors, *IEEE transactions on robotics and automation, Vol.15, No.6, December 1999. pp.1116-1121.*

Xiaolin Zhong, John Lewis etc., 1996. Inverse Robot Calibration Using Artificial neural Networks, *Engng Applic. Artif. Intell. Vol. 9, No. 1, pp. 83-93.*

Yu Liu, Bin Liang et al., 2007. Calibration of a Steward Parallel Robot Using Genetic Algorithm, *Proceedings of the 2007 IEEE International Conference on Mechatronics and Automation, August 5-8, 2007, Harbin,China. pp. 2495-2500.*